

# Tuning the Thermoelectric Properties of Ferrocene Molecular Junctions

Mohammed D Noori<sup>a</sup>, Alaa A Al-Jobory<sup>b</sup>

<sup>a</sup>Physics department, college of science, University of Thi Qar, Iraq

<sup>b</sup>Physics department, College of Education for Pure Science, University of Anbar, Anbar, Iraq

**Abstract.** The calculations of thermoelectric and transport properties have been carried out by using the SIESTA implementation of density functional theory (DFT), with a generalized gradient functional approximation (GGA-PBE) for the exchange and correlation functionals. In this work we have compared the thermoelectric properties of FeCP with two different configurations. The results show that the spin-dependent transport properties can be affected by the molecular structure and the substitution of the terminal thiol groups plays an important role on the spin-dependent transmission of the molecular junctions. Meanwhile, electrical conductance and thermal conductance also affected. The thermoelectric properties of Ferrocene (FeCp<sub>2</sub>) for these two different configurations have been compared. Thus, all these transport properties are combined to produce a good value of the room-temperature figure of merit ZT.

**Keywords:** ferrocene, density functional theory, spin polarization, and seebeck coefficient

## 1. Introduction

Molecular electronics is the field where the electrical properties of a single molecule are exploited to form an electronic junction. Many researches in the molecular electronics field have so far mostly concentrated on dc electrical contacts. Nowadays it is known as charge transport through organic molecules. Investigations of charge transport through single molecules are of fundamental interest and are relevant to the proposed future applications of molecules in next-generation electronic devices [1-4].

Recently, molecular electronics have a great interest from both a theoretical and an applied electronics point of view, they have much interest in the develop and control electronic molecules that can exploit as the active elements in future nano-electronic circuits components among which one can mention molecular wires [5,6], electrodes [7,8], spreaders [9], interconnectors [10], magnets [11-13], switches [14,15] and rectifiers [16-19]. Recently, scientists have studied the possibility of conversion of generated thermal energy to electrical energy by thermoelectric properties of the devices [20-24]. So, the investigation and focusing on thermoelectric properties of the molecular junction has been of interest lately from two aspects- saving energy and power generation. The nanostructures show significantly thermal properties to make them good candidates for the design of the next generation of integrated electronics devices. The efficiency of thermoelectric materials is determined by their thermoelectric figure of merit ( $ZT = S^2GT / \kappa$ ) where S is the Seebeck coefficient, G is the electrical conductance, T is the temperature and  $\kappa$  is the electronic thermal conductivity. Among various of these metal complexes, metallocene's such as ferrocene and cobaltocene are currently investigated as a good candidate for constructing molecular devices and also due to they possess high chemical and thermal stability and unpaired spin components. Therefore, Metallocenes is a complex with a transition metal



cation sandwiched between cyclopentadienyl (Cp) rings. Whereas, Ferrocene ( $\text{FeCp}_2$ ) is one of the most common metallocene it consists of two (Cp) rings bound by a central iron atom. The two Cp rings in ferrocene show two different conformations where these two Cp rings can be in the staggered or eclipsed conformation and rotate around the Cp-Fe-Cp axis with low resistance.

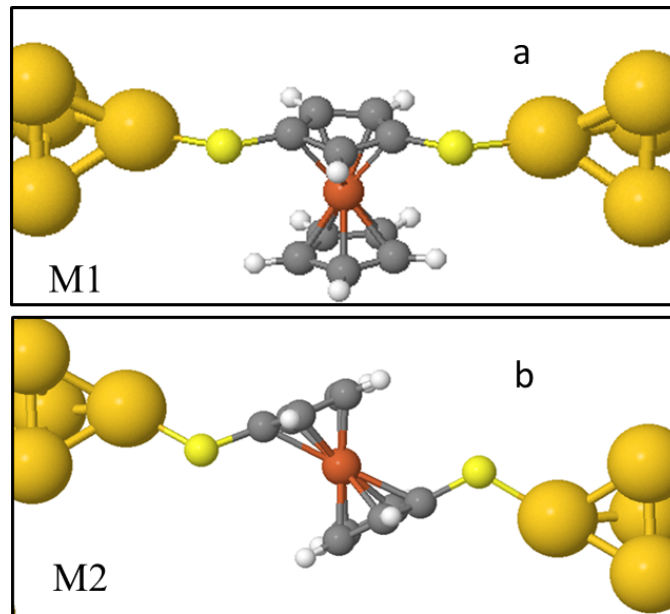


**Figure 1.** The optimized geometries of the thiolated-terminated ferrocene in two different configurations M1 (a) and M2 (b)

In this paper, as shown above in figure 1, the effect of molecular structure on the spin-dependent transport and thermoelectric properties of the two structures M1 and M2 of ferrocene sandwiched between two gold electrodes are investigated. The calculations of quantum transport properties have been carried out by using the SIESTA [25] implementation of density functional theory (DFT), with a generalized gradient functional approximation (GGA-PBE) for the exchange and correlation functionals [26,27].

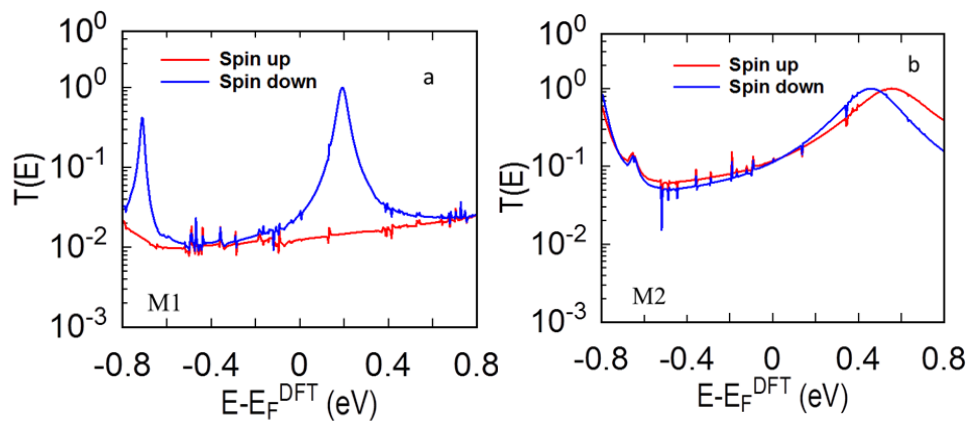
## 2. Computational Method

Figure 1 illustrates the structures of the two molecular junctions employed in this work; they labeled M1 and M2 respectively. The ferrocene molecule is sandwiched between two gold electrodes via a pair of sulfur atoms. Firstly, the molecular geometry in figure 1 is optimized before building the junction model. Then, the geometry of each structure consisting of the gold electrodes and a single molecule (Ferrocene) which was relaxed to a force tolerance of  $20 \text{ meV}/\text{\AA}$  using the SIESTA [25] implementation of density functional theory (DFT), with a double- $\zeta$  polarized basis set (DZP) and generalized gradient functional approximation (GGA-PBE) for the exchange and correlation functionals. To calculate the electronic and thermoelectric properties of the molecules in the junction, from the converged DFT calculation, the underlying mean-field Hamiltonian  $H$  was combined with our quantum transport code, GOLLUM [28] to calculate the transmission coefficient  $T_{el}(E)$  for electrons of energy  $E$  passing from the source to the drain. The electrical conductance  $G_{el}(T) = G_0 L_0$ , the electronic contribution of the thermal conductance  $\kappa_{el}(T) = (L_0 L_2 - L_1^2)/h T L_0$ , and the thermopower  $S(T) = -L_1/e T L_0$  of the junction are calculated from the electron transmission coefficient  $T_{el}(E)$  where  $L_n(T) = \int_{-\infty}^{\infty} dE (E - E_F)^n T_{el}(E) \left( -\frac{\partial f_{FD}(E,T)}{\partial E} \right)$  and  $f_{FD}(E,T)$  is the Fermi-Dirac probability distribution function  $f_{FD}(E,T) = (e^{(E-E_F)/k_B T} + 1)^{-1}$ ,  $T$  is the temperature,

$E_F$  is the Fermi energy,  $G_0 = 2e^2/h$  is the conductance quantum,  $e$  is electron charge, and  $h$  is the Planck's constant.

### 3. Results and discussion

Regarding structures M1 and M2 of figure 1, we employed the SIESTA [25] implementation of spin-polarized density functional theory (DFT) and from the converged mean field DFT Hamiltonian, and by using quantum transport code, GOLLUM to compute the electronic transmission coefficient  $T_{\sigma el}(E)$  for electrons with energy  $E$  and spin  $\sigma = [\uparrow, \downarrow]$  passing from one electrode to the other through the ferrocene. Figure 2a below shows that the transmission coefficient of spin up and spin down states in energy windows  $[-0.8, 0.8]$  eV in junction M1, the transmission coefficient of spin up and spin down as a function of the energy for the same range have been shown in figure 2b for M2 junction. Figure 2b shows there is little difference for the transmission coefficient between spin up and spin down states at this range of energy, whereas figure 2a shows that there is a remarkable difference between spin up and spin down states at the same range of energy. Contrary to structure M1, Fe atom in structure M2 may make a more participation to the electron tunneling from one electrode to the other electrode passing through the molecule. However, the conductivity is enhanced accordingly. Therefore, our results indicate that the contribution of Fe atom plays an essential role in the molecular conductance.



**Figure 2.** Transmission coefficients as a function of energy, spin up (red line) and spin down (blue line), (a) for M1 and (b) for M2.

Figure 3 below shows the total spin-dependent transmissions  $T_{\sigma el}(E)$  for M1 and M2 junctions, whereas the corresponding room-temperature conductance versus Fermi energy  $E_F$  are shown in figure 4. However, figure 4 shows that the conductance of M2 junction is higher than the conductance of an M1 junction for the whole range except around  $E_F=0.2$  eV. Figure 5 shows that the thermal conductance due to the electrons  $\kappa_{el}$  of M2 higher than M1 for a wide range of energy in the vicinity of DFT predicted Fermi energy.

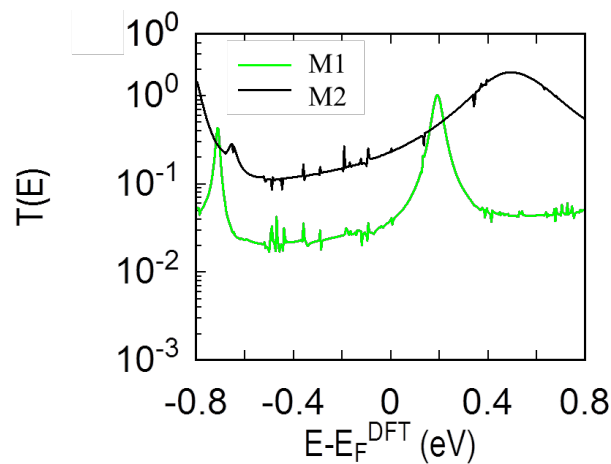


**Figure 3.** Total transmission coefficients as a function of energy (green line) for M1 configuration and (black line) for M2 configuration

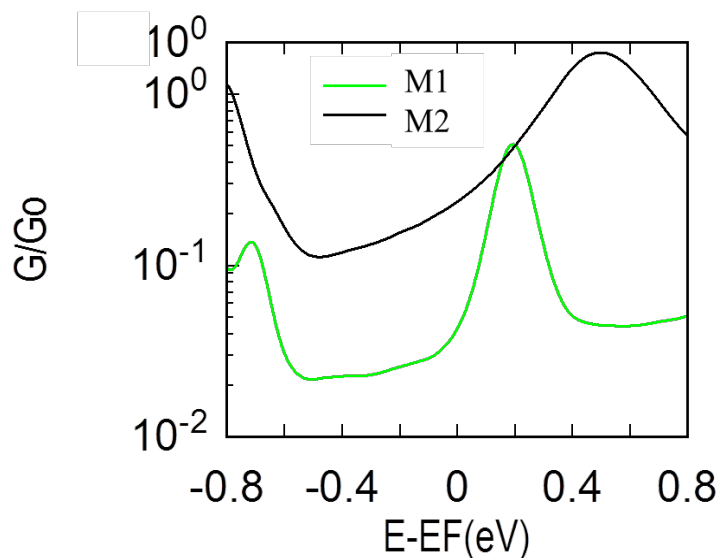


**Figure 4.** Electrical conductance as a function of energy (green line) for M1 configuration and (black line) for M2 configuration

To examine the thermoelectric properties of M1 and M2, we obtained the Seebeck coefficient of both structures from the electron transmission coefficient  $T_{el}(E)$ , as described in the Methods. Figure 6 shows the Seebeck coefficients as a function of Fermi energy  $E_F$ . Figure 6 demonstrates that both the magnitude and sign of  $S$  are sensitive to configuration of the junction and reveals that M1 has a large negative and positive values comparing with M2 which shows almost flat curve and this due to the higher slope of  $\ln T_{el}(E_F)$  of M1 over a wide range of Fermi energies between the HOMO and LUMO. Since the electronic thermal conductance is higher in M2, the electrical conductance is proportional to the electronic thermal conductance. Consequently, as shown in figure 7, due to the high Seebeck coefficient of M1, a  $ZT$  as high as 0.8 eV is obtained when  $E_F$  lies in an energy window in the vicinity of the DFT-predicted Fermi energy. Although both of these structures are consist of (FeCp2), our study suggests that the importance of the molecular configurations on the thermoelectrical properties in (FeCp2) molecular junctions.

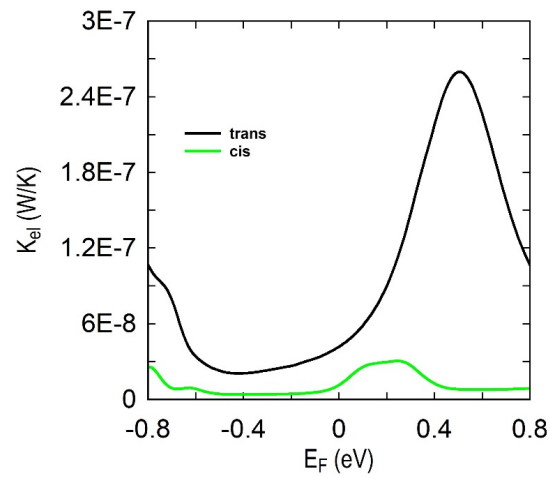


**Figure 5.** Thermal conductance as a function of energy (green line) for M1 configuration and (black line) for M2 configuration

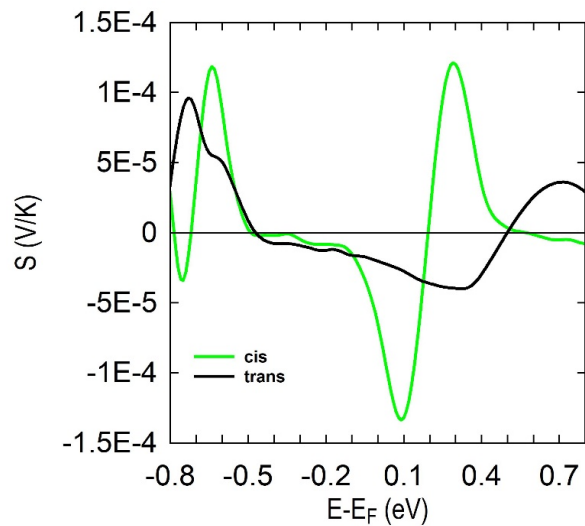


**Figure 6.** Thermopower  $S$  as a function of energy (green line) for M1 configuration and (black line) for M2 configuration

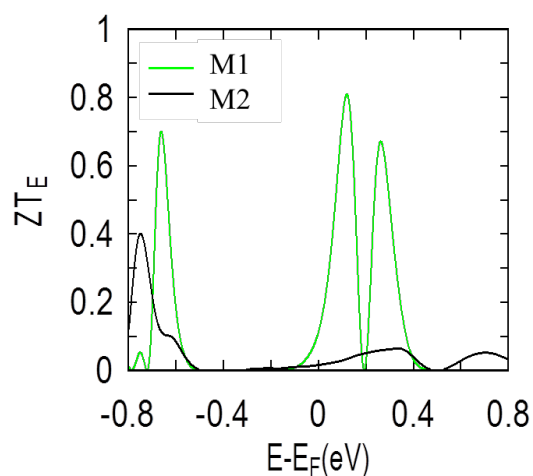


**Figure 7.** Figure of merit  $ZT$  as a function of energy (green line) for M1 configuration and (black line) for M2 configuration

#### 4. Conclusions

In this work, the spin-dependent transport properties of the molecular junctions based on ferrocene with terminal thiol groups are investigated by theoretical simulation. regarding the two models M1 and M2, the calculated results showed that the spin-dependent transport properties can be affected by the molecular structure. The substitution of the terminal thiol groups plays an important role on the spin-dependent transmission and the total transmission of the molecular junctions. The total transmission values, electrical conductance and thermal conductance in M1 are all less than those in M2. Additionally, we have compared the thermoelectric properties of Ferrocene ( $\text{FeCp}_2$ ) for M1 and M2 and found that the M1 has a high Seebeck coefficient comparing with M2. These transport properties combine to yield a room-temperature figure of merit of  $ZT \sim 0.8$  for M1 structure.

#### 5. References

1. N. Weibel, S. Grunder and M. Mayor, *Organic & biomolecular chemistry*, 2007, **5**, 2343-2353.
2. S. J. van der Molen and P. Liljeroth, *Journal of Physics: Condensed Matter*, 2010, **22**, 133001.
3. S. V. Aradhya and L. Venkataraman, *Nature nanotechnology*, 2013, **8**, 399.
4. J. A. Malen, S. K. Yee, A. Majumdar and R. A. Segalman, *Chemical Physics Letters*, 2010, **491**, 109-122.
5. R.-W. Yan, X. Jin, S.-Y. Guan, X.-G. Zhang, R. Pang, Z.-Q. Tian, D.-Y. Wu and B.-W. Mao, *The Journal of Physical Chemistry C*, 2016, **120**, 11820-11830.
6. K. H. Khoo, Y. Chen, S. Li and S. Y. Quek, *Physical Chemistry Chemical Physics*, 2015, **17**, 77-96.
7. P. Tyagi, D. Li, S. M. Holmes and B. J. Hinds, *Journal of the American Chemical Society*, 2007, **129**, 4929-4938.
8. G. Schull, T. Frederiksen, A. Arnau, D. Sánchez-Portal and R. Berndt, *Nature Nanotechnology*, 2010, **6**, 23.

9. H. Han, Y. Zhang, N. Wang, M. K. Samani, Y. Ni, Z. Y. Mijbil, M. Edwards, S. Xiong, K. Sääskilähti, M. Murugesan, Y. Fu, L. Ye, H. Sadeghi, S. Bailey, Y. A. Kosevich, C. J. Lambert, J. Liu and S. Volz, *Nature Communications*, 2016, **7**, 11281.
10. F.-P. Lu, Q. Wang and X. Zhou, *Chinese Physics B*, 2013, **22**, 037202.
11. D. Luneau, *Current Opinion in Solid State and Materials Science*, 2001, **5**, 123-129.
12. A. Caneschi, D. Gatteschi and F. Totti, *Coordination Chemistry Reviews*, 2015, **289-290**, 357-378.
13. L. Bogani and W. Wernsdorfer, *Nature Materials*, 2008, **7**, 179.
14. B. L. Feringa, R. A. van Delden, N. Koumura and E. M. Geertsema, *Chemical Reviews*, 2000, **100**, 1789-1816.
15. H. Li and D.-H. Qu, *Science China Chemistry*, 2015, **58**, 916-921.
16. A. Aviram and M. A. Ratner, *Chemical Physics Letters*, 1974, **29**, 277-283.
17. C. Van Dyck and M. A. Ratner, *Nano Letters*, 2015, **15**, 1577-1584.
18. N. J. Geddes, J. R. Sambles and A. S. Martin, *Advanced Materials for Optics and Electronics*, 2004, **5**, 305-320.
19. A. Dhirani, P. H. Lin, P. Guyot-Sionnest, R. W. Zehner and L. R. Sita, *The Journal of Chemical Physics*, 1997, **106**, 5249-5253.
22. M. Noori, H. Sadeghi, Q. Al-Galiby, S. W. Bailey and C. J. Lambert, *Physical Chemistry Chemical Physics*, 2017, **19**, 17356-17359.
23. M. Noori, H. Sadeghi and C. J. Lambert, *Nanoscale*, 2017, **9**, 5299-5304.
24. M. Noori, A. C. Aragonès, G. Di Palma, N. Darwish, S. W. Bailey, Q. Al-Galiby, I. Grace, D. B. Amabilino, A. González-Campo and I. Díez-Pérez, *Scientific reports*, 2016, **6**, 37352.
25. J. M. Soler, E. Artacho, J. D. Gale, A. García, J. Junquera, P. Ordejón and D. Sánchez-Portal, *Journal of Physics: Condensed Matter*, 2002, **14**, 2745.
26. J. P. Perdew, K. Burke and M. Ernzerhof, *Physical Review Letters*, 1996, **77**, 3865.
27. B. Hammer, L. B. Hansen and J. K. Nørskov, *Physical review B*, 1999, **59**, 7413.
28. J. Ferrer, C. J. Lambert, V. M. Garcia-Suarez, D. Z. Manrique, D. Visontai, L. Oroszlany, R. Rodriguez-Ferradas, I. Grace, S. W. D. Bailey, K. Gillemot, H. Sadeghi and L. A. Algharagholy, *New Journal of Physics*, 2014.